MAGI-2 orchestrates the localization of backbone proteins in the slit diaphragm of podocytes

OPEN

Hiroyuki Yamada[1,2,3,10], Naritoshi Shirata[3,4,10], Shinichi Makino[1,2,3], Takafumi Miyake[2,3], Juan Alejandro Oliva Trejo[3], Kanae Yamamoto-Nonaka[2,3], Mitsuhiro Kikyo[3,4], Maulana A. Empitu[1], Ika N. Kadariswantiningsih[1], Maiko Kimura[1], Koichiro Ichimura[5], Hideki Yokoi[2], Masashi Mukoyama[6], Akitsu Hotta[7], Katsuhiko Nishimori[8], Motoko Yanagita[2,3,9] and Katsuhiko Asanuma[1,3]

[1]Department of Nephrology, Graduate School of Medicine, Chiba University, Chiba, Japan; [2]Department of Nephrology, Graduate School of Medicine, Kyoto University, Kyoto, Japan; [3]Medical Innovation Center, TMK Project, Graduate School of Medicine, Kyoto University, Kyoto, Japan; [4]Sohyaku, Innovative Research Division, Mitsubishi Tanabe Pharmaceutical Corporation, Saitama, Japan; [5]Department of Anatomy and Life Structure, Juntendo University Graduate School of Medicine, Tokyo, Japan; [6]Department of Nephrology, Kumamoto University Graduate School of Medical Sciences, Kumamoto, Japan; [7]Department of Reprogramming Science, Center for iPS Cell Research and Application (CiRA), Kyoto University, Kyoto, Japan; [8]Department of Obesity and Inflammation Research, Fukushima Medical University, Fukushima, Japan; and [9]Institute for the Advanced Study of Human Biology (ASHBi), Kyoto University, Kyoto, Japan

Podocytes are highly specialized cells within the glomerulus that are essential for ultrafiltration. The slit diaphragm between the foot processes of podocytes functions as a final filtration barrier to prevent serum protein leakage into urine. The slit-diaphragm consists mainly of Nephrin and Neph1, and localization of these backbone proteins is essential to maintaining the integrity of the glomerular filtration barrier. However, the mechanisms that regulate the localization of these backbone proteins have remained elusive. Here, we focused on the role of membrane-associated guanylate kinase inverted 2 (MAGI-2) in order to investigate mechanisms that orchestrate localization of slit-diaphragm backbone proteins. MAGI-2 downregulation coincided with a reduced expression of slit-diaphragm backbone proteins in human kidneys glomerular disease such as focal segmental glomerulosclerosis or IgA nephropathy. Podocyte-specific deficiency of MAGI-2 in mice abrogated localization of Nephrin and Neph1 independently of other scaffold proteins. Although a deficiency of zonula occuldens-1 downregulated the endogenous Neph1 expression, MAGI-2 recovered Neph1 expression at the cellular edge in cultured podocytes. Additionally, overexpression of MAGI-2 preserved Nephrin localization to intercellular junctions. Co-immunoprecipitation and pull-down assays also revealed the importance of the PDZ domains of MAGI-2 for the interaction between MAGI-2 and slit diaphragm backbone proteins in podocytes. Thus, localization and stabilization of Nephrin and Neph1 in intercellular junctions is regulated mainly via the PDZ domains of MAGI-2 together with other slit-diaphragm scaffold proteins. Hence, these findings may elucidate a mechanism by which the backbone proteins are maintained.

Kidney International (2021) **99,** 382–395; https://doi.org/10.1016/j.kint.2020.09.027

KEYWORDS: FSGS; MAGI-2; MAGI2; nephrin; neph1; podocyte

Translational Statement

To prevent proteinuria, it is necessary to preserve the slit diaphragm (SD) of podocytes, which functions as a final glomerular filtration barrier. However, what is important to protect nephrin and neph1—the main components of the SD—remains unknown. Investigations using podocyte-specific MAGI-2 knockout mice have shown that MAGI-2 is indispensable for the proper localization of nephrin and neph1. In a human kidney with focal segmental glomerulosclerosis and IgA nephropathy, MAGI-2 downregulation coincides with a reduced expression of the backbone proteins of the SD. Hence, a MAGI-2 protection strategy could be an effective new route to the development of drugs that could prevent proteinuria.

Podocytes are highly differentiated pericyte-like cells that wrap themselves around the capillary loops in glomeruli.[1] The differentiated cells consist of a cell body, major processes, and many foot processes. In the intercellular space between foot processes, there is a fine membrane structure called a slit diaphragm (SD).[2] Along with the glomerular basement membrane, this fine membrane functions as a filtration barrier to prevent the passage of plasma proteins into the urinary filtrate.[3–5]

Correspondence: *Katsuhiko Asanuma, Department of Nephrology, Graduate School of Medicine, Chiba University, 1-8-1 Inohana, Chuo-ku, Chiba 260-8670, Japan. E-mail: kasanuma@chiba-u.jp*

[10]HY and NS contributed equally to this work.

Received 13 December 2019; revised 22 August 2020; accepted 10 September 2020; published online 2 November 2020

Nephrin and neph1 are known as the backbone proteins of the SD in podocytes. A failure to maintain these backbone proteins of the SD is believed to be the basis of proteinuria.[6,7] In fact, a large body of evidence has shown that the deletion of these backbone proteins induces focal segmental glomerulosclerosis (FSGS).[5,8–10] Many genetic analyses have also revealed the importance of these gene mutations in the development of nephrotic syndrome in humans.[11–20] Thus, we were compelled to elucidate how these backbone proteins are physiologically localized and preserved in podocytes. Scaffold proteins such as podocin, CD2-associated protein, and zonula occludens-1 (ZO-1) are reported to be involved in stabilizing these backbone proteins.[21–25] However, it has remained unclear how nephrin and neph1 are localized in the intracellular junctions of podocytes and whether other scaffold proteins are also involved in the SD maintenance.

Membrane-associated guanylate kinase inverted 2 (MAGI-2) is also 1 of the scaffold proteins identified in neuronal spines and podocytes.[26–28] It has already been established that MAGI-2 mediates the signaling of G-protein–coupled receptors, Ras homolog family member A, and Ras-associated protein 1.[29–31] We previously reported that podocyte-specific MAGI-2 knockout (KO) mice exhibit glomerulosclerosis and kidney failure in a manner similar to FSGS.[32] Other studies also have revealed that MAGI-2 genetic mutation leads to a severe renal phenotype in mice and humans.[30,33–36] However, an understanding of the mechanism underlying the phenotype has remained elusive. In particular, although the SD in podocytes is crucial as a kidney filtration barrier, it is unclear whether MAGI-2 interacts with the SD. In fact, other groups have also shown that MAGI-2 does not bind to nephrin.[37,38] The question of whether MAGI-2 acts as a scaffold protein to bolster SD proteins such as nephrin and neph1 has been shrouded in controversy for decades.

In this study, we describe the function of MAGI-2 to show how the localization of nephrin and neph1 could be stabilized in the plasma membrane.

RESULTS

MAGI-2 is downregulated alongside a key component of the SD in experimental nephritis models

MAGI-2 has already been identified as a component of the SD complex.[27] To provide precise subcellular localization of MAGI-2, we used post-embedding immunoelectron microscopy of a rat kidney and detected the MAGI-2 signal at the cytoplasmic insertion of the SD into the foot process (Figure 1a).

To investigate the dynamic expression of MAGI-2 under pathologic conditions, we established an experimental nephrosis model of doxorubicin (Adriamycin)-induced nephropathy, which is regarded as an equivalent model for human FSGS.[39] Adriamycin mice exhibited massive albuminuria 7 days after Adriamycin injection (Supplementary Figure S1A). Immunofluorescence analysis showed that the expressions of nephrin and neph1, key components of SDs, were reduced in the glomeruli on day 7, along with the expression of MAGI-2 (Supplementary Figure S1B).

We then investigated a puromycin aminonucleoside nephropathy rat model, which is another nephrosis model.[39] This model also showed massive proteinuria at days 7 and 14 after Adriamycin injection (Supplementary Figure S1C). MAGI-2, nephrin, and neph1 expressions were also simultaneously downregulated (Supplementary Figure S1D). Thus, these results suggested the possibility that MAGI-2 interacts with nephrin and neph1 in a manner similar to that of other scaffold proteins.

MAGI-2 podocyte-specific KO mice show decreased expressions of nephrin and neph1

We previously generated congenital podocyte-specific MAGI-2 KO (MAGI-2 pdKO) mice.[32,40] Our data showed that MAGI-2 pdKO mice exhibited massive albuminuria and severe glomerulosclerosis at 8 weeks of age.[32] In additional, all MAGI-2 pdKO mice died by 20 weeks due to renal failure.

In this study, using MAGI-2 pdKO mice, we intended to investigate whether MAGI-2 could influence the localization of SD proteins. In the control mice, nephrin and neph1 were distributed in the capillary pattern of glomeruli (Figure 1b and 1c). In contrast, as high-magnification images show, the nephrin staining of MAGI-2 pdKO mice exhibited a cytosolic pattern at 4 and 8 weeks (Figure 1b). Also, Western blots of glomerular lysates showed that the expressions of nephrin and neph1 were dramatically decreased in MAGI-2 pdKO mice from 4 weeks of age (Figure 1d).

Meanwhile, the expression of podocin, which interacts with nephrin, was not downregulated in MAGI-2 pdKO mice, although its immunostaining pattern was altered (Figure 1c and 1d). Also, the expression difference in ZO-1, a scaffold protein of neph1,[23] was not as apparent as that in neph1 (Figure 1c and 1d). Moreover, our previous study has shown that the expression of CD2-associated protein, a scaffold protein of nephrin, is at the same level in both groups.[32] These results show that MAGI-2 deletion altered the expression of nephrin and neph1, although that of other scaffold proteins was sustained. These results also indicate that MAGI-2 is important for the proper localization and steady-state abundance of nephrin and neph1 similar to that of other scaffold proteins.

An acquired deletion of MAGI-2 can also cause proteinuria and glomerulosclerosis

Investigations with MAGI-2 pdKO mice revealed evidence supporting the hypothesis that MAGI-2 regulates the localization of SD key components. However, we could not deny that the reduced SD expression in MAGI-2 pdKO mice simply reflects glomerulosclerosis, because these mice exhibited sclerotic lesions from 8 weeks of age. In additional, Cre/loxP-mediated deletion could have a substantial impact on SD-associated genes during developmental stages.

To eliminate these concerns, we generated inducible podocyte-specific MAGI-2 knockout (MAGI-2 IpdKO) mice

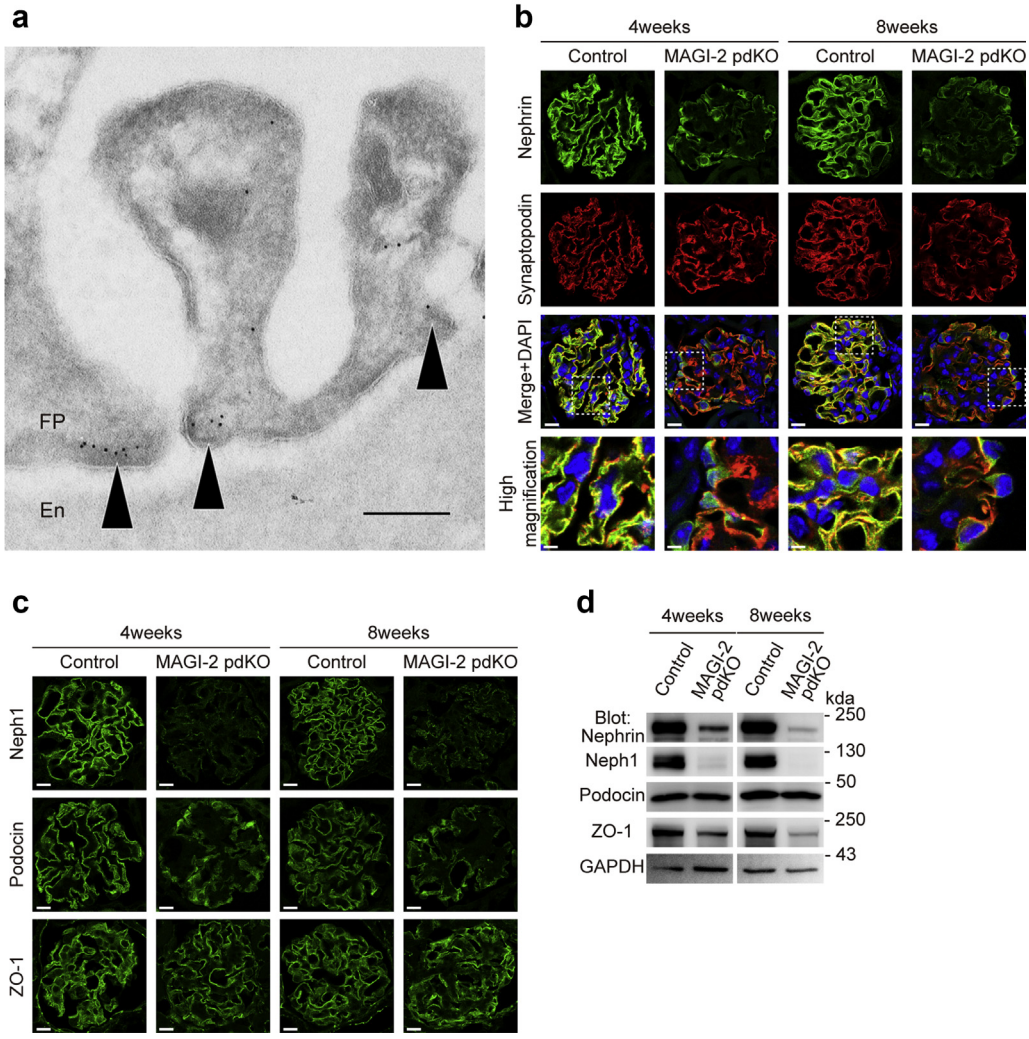

Figure 1 | Podocyte-specific MAGI-2 KO mice showed the downregulated expression of slit diaphragm backbone proteins. (**a**) Representative immunoelectron microscopic image of a rat glomerulus. The arrowhead indicates a MAGI-2 immunologic signal. Bar = 200 nm. (**b**) Representative glomerular immunofluorescence images of nephrin (green) and synaptopodin (red) in control and MAGI-2 pdKO mice at ages of 4 and 8 weeks. The white doted boxes indicate high magnification. Bars = 6 μm and 20 μm. (**c**) Representative glomerular immunofluorescence images of neph1, podocin, and ZO-1 in control and MAGI-2 pdKO mice at ages of 4 and 8 weeks. Bar = 20 μm. (**d**) Western blot analysis for nephrin, podocin, neph1, and ZO-1 expressions in the glomerular lysate of control and MAGI-2 pdKO mice at ages of 4 and 8 weeks. DAPI, 4′,6-diamidino-2-phenylindole; En, endothelial cell; FP, foot process; GAPDH, glyceraldehyde-3-phosphate dehydrogenase; MAGI-2 pdKO, MAGI-2 podocyte-specific knockout; ZO-1, zonula occludens-1. To optimize viewing of this image, please see the online version of this article at www.kidney-international.org.

by crossing MAGI-2$^{flox/flox}$ mice with NPHS2-CreER^{T2} mice[41] (Figure 2a). Four weeks after the MAGI-2 IpdKO mice received an injection of tamoxifen, a Western blot of glomerular lysates and immunofluorescence demonstrated MAGI-2 downregulation (Figure 2b and 2c).

Twenty weeks after a tamoxifen injection, MAGI-2 IpdKO mice also exhibited significantly massive proteinuria (0.03 g/gCre vs. 2.40 g/gCre, $P < 0.05$; Figure 2d). Six months after the injection, periodic acid–Schiff staining of the kidney specimens in MAGI-2 IpdKO mice revealed sclerotic lesions, whereas no sclerotic lesions were observed in the control mice (Figure 2e). The glomerulosclerosis index in MAGI-2 IpdKO mice was significantly higher (0 vs. 5.8 %, $P = 0.03$; Supplementary Figure S2A). In fact, the immunofluorescence of *WT-1*, a marker for the podocyte nucleus, revealed that the number of podocyte nuclei is significantly lower in MAGI-2 IpdKO mice (Supplementary Figure S2B and S2C). This result indicates that the podocytes are more detached in the MAGI-2 IpdKO group. In addition, electron microscopy showed an abnormal morphology for the podocyte ultrastructure in MAGI-2 IpdKO mice (Figure 2f and g). These results again supported the finding that MAGI-2 deletion leads to proteinuria and glomerulosclerosis.

Acquired MAGI-2 deletion causes a reduced expression of nephrin and neph1 independently of other scaffold proteins

To investigate the MAGI-2 function for SD components, we next analyzed the expression change in the SD components 3 weeks after tamoxifen injection and found that MAGI-2 expression was simply downregulated in MAGI-2 IpdKO

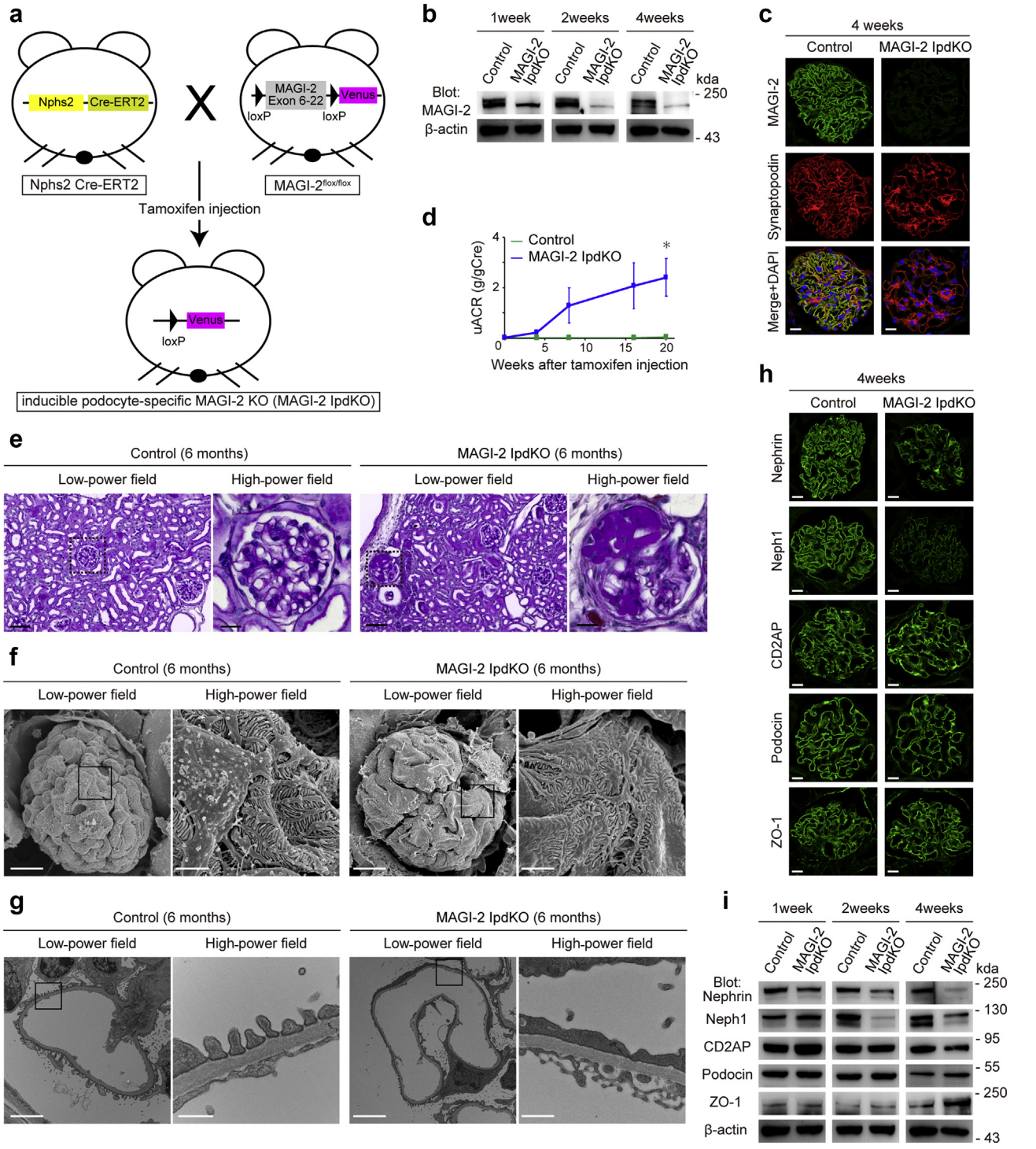

Figure 2 | Inducible podocyte-specific MAGI-2 KO mice also showed proteinuria and decreased expression of slit-diaphragm proteins. (**a**) Brief outline of the breeding methods for inducible podocyte-specific MAGI-2 knockout (MAGI-2 IpdKO) mice. (**b**) Western blot analysis for MAGI-2 expression in the glomerular lysate of control and MAGI-2IpdKO mice 1, 2, and 4 weeks after tamoxifen injection. (**c**) Representative glomerular immunofluorescence images of MAGI-2 (green) and synaptopodin (red) in control and MAGI-2 IpdKO mice 4 weeks after tamoxifen injection. Bar = 20 μm. (**d**) Urinary albumin-to-creatinine ratio of control and MAGI-2 IpdKO mice; $^*P < 0.05$. (**e**) Representative glomerular periodic acid–Schiff staining images in control and MAGI-2 IpdKO mice 6 months after tamoxifen injection. Bar = 20 μm. (**f**) Scanning electron microscope images in control and MAGI-2 IpdKO mice 6 months after tamoxifen injection. The black boxes indicate high-power fields. Bars of low- and high-power fields = 20 and 2.0 μm, respectively. (**g**) Transmission electron microscope images in control and MAGI-2 IpdKO mice 6 months after tamoxifen injection. The black boxes indicate high-power field (Bars of the low- and high-power fields = 2.0 μm and 500 nm, respectively. (**h**) Representative glomerular immunofluorescence images of Nephrin, Neph1, CD2AP, podocin, and ZO-1 in control and MAGI-2 IpdKO mice 4 weeks after tamoxifen injection. Bar = 20 μm. (**i**) Western blot analysis for nephrin, (continued)

mice, whereas little proteinuria or few sclerotic lesions were seen in the control group (Figure 2b and d).

Immunofluorescence showed that the expressions of nephrin and neph1 were downregulated in MAGI-2 IpdKO mice, although there were no apparent differences in other scaffold proteins, such as CD2-associated protein, ZO-1, and podocin (Figure 2h). In addition, the staining of nephrin in MAGI-2 IpdKO mice adopted a cytosolic pattern, whereas a capillary pattern was retained in the control mice. Similarly, a Western blot of glomeruli showed that the nephrin and neph1 expressions began to decrease from 2 weeks after tamoxifen injection in a manner similar to that of MAGI-2 (Figure 2i). Meanwhile, there were no evident differences in the expressions of other scaffold proteins within these time frames. These results show that the acquired deletion of MAGI-2 results in a reduced expression of the SD main components, which supports the hypothesis that MAGI-2 may maintain localization of the SD main components similar to other scaffold proteins.

ZO-1 deletion in cultured podocytes undermines neph1 expression

In the previous sections, our results showed that MAGI-2 expression is necessary to maintain the apparent abundance of neph1 in this experimental context. Meanwhile, prior studies have demonstrated that ZO-1 also supports the neph1 structure as a scaffold protein.[23,42] This interaction between neph1 and ZO-1 has been adequately demonstrated in biochemical assays and in *in vitro* and *in vivo* studies.[23,42,43] Hence, we investigated the interaction among neph1, ZO-1, and MAGI-2 using conditionally immortalized podocyte cell lines. First, because neph1 and ZO-1 are expressed in cultured differentiated podocytes (Figure 3a and b), we established cultured ZO-1 KO podocytes via a clustered regularly interspaced short palindromic repeats (CRISPR)–Cas9 gene-editing system (CRISPR Therapeutics, Cambridge, MA) (Figure 3c).[44] Sanger sequence analysis of the KO cell line revealed 5 base pair deletions in the target sequence (Figure 3d).

Immunofluorescence analysis showed that the ZO-1 expression was not observed in the cell-cell interface in ZO-1 KO podocytes, but it remained detectable in control podocytes (Figure 3e). In ZO-1 KO podocytes, the neph1 expression also vanished in the cell-cell contact area but remained unchanged in control podocytes (Figure 3f). Other ZO-1 KO cell lines also showed similar phenomena (Supplementary Figure S3A and B). Western blot analysis of these cell lysates showed that the neph1 expression in ZO-1 KO podocytes was significantly lower compared with the control and wild-type (WT) podocytes (Figure 3g and 3h). These results provide further evidence that ZO-1 is essential for maintaining the neph1 expression in podocytes.

One possible reason for the neph1 downregulation in ZO-1 KO podocytes might have been the off-target mutations after the CRISPR-Cas9 system. However, no mutations were detected in these off-target candidate sites (Supplementary Figure S4A). In addition, the mRNA expression of neph1 was not significantly different among these cell lines (Supplementary Figure S4B). These results suggest little possibility that neph1 downregulation is due to off-target mutagenesis.

Based on these results, we considered that ZO-1 deletion leads to neph1 degradation due to an unstable condition because ZO-1 is a scaffold protein of neph1.[23] Then, to clarify how neph1 was degraded in ZO-1 KO podocytes, we examined the potential degradation pathway of neph1 in ZO-1 KO podocytes by administering inhibitors of either protease or proteasome. The neph1 expression in ZO-1 KO podocytes was elevated in the bortezomib administration group (Supplementary Figure S4C). Thus, these results indicated that ZO-1 deficiency induces instability in neph1 localization, which leads to neph1 degradation via the ubiquitin-proteasome pathway.

MAGI-2 could rescue neph1 abundance in cultured ZO-1 KO podocytes

As suggested by the finding in MAGI-2 IpdKO mice, MAGI-2 may regulate neph1 expression. However, MAGI-2 is not expressed in the cultured podocytes (Figure 3a). Thus, the phenomena of diminishing neph1 expression in ZO-1 KO podocytes were observed in the absence of MAGI-2. To investigate the role of MAGI-2 in stabilizing neph1, we needed to transfect MAGI-2 transiently to cultured ZO-1 KO podocytes. In reality, however, the efficacy of lipofection methods for transfecting cultured differentiated podocytes is quite low. Hence, we examined the possibility of using a super electroporator, NEPA21 (Nepa Gene, Chiba, Japan) and green fluorescence protein (GFP)–control plasmid DNA to transfect cultured differentiated podocytes (Supplementary Table S1). After optimizing the conditions, this instrument provided high transfection efficiency and viability of cultured differentiated podocytes compared with conventional lipofection methods (Supplementary Figure S5A).

With an optimized process of electroporation in hand, MAGI-2 was expressed at the cellular edge of ZO-1 KO podocytes but was not detected in control podocytes (Figure 3i). Then the endogenous neph1 expression returned to the cellular edge in ZO-1 KO podocytes with the overexpression of MAGI-2 (Figure 3j). Meanwhile, the neph1 expression remained undetectable in the ZO-1 KO podocytes with an empty vector. Western blot of these cell lysates also showed that the neph1 expression in ZO-1 KO podocytes with MAGI-2 could be re-established as strong as that of the wild type (Figure 3k and l). Our analysis demonstrated that, together with ZO-1, MAGI-2 also plays a central role in neph1 localization and expression as a scaffold protein.

Figure 2 | (continued) neph1, CD2AP, podocin, and ZO-1 expression in the glomerular lysate of control and MAGI-2 IpdKO mice 1, 2, and 4 weeks after tamoxifen injection. CD2AP, CD2 associated protein; uACR, urinary albumin-to-creatinine ratio; ZO-1, zonula occludens-1. To optimize viewing of this image, please see the online version of this article at www.kidney-international.org.

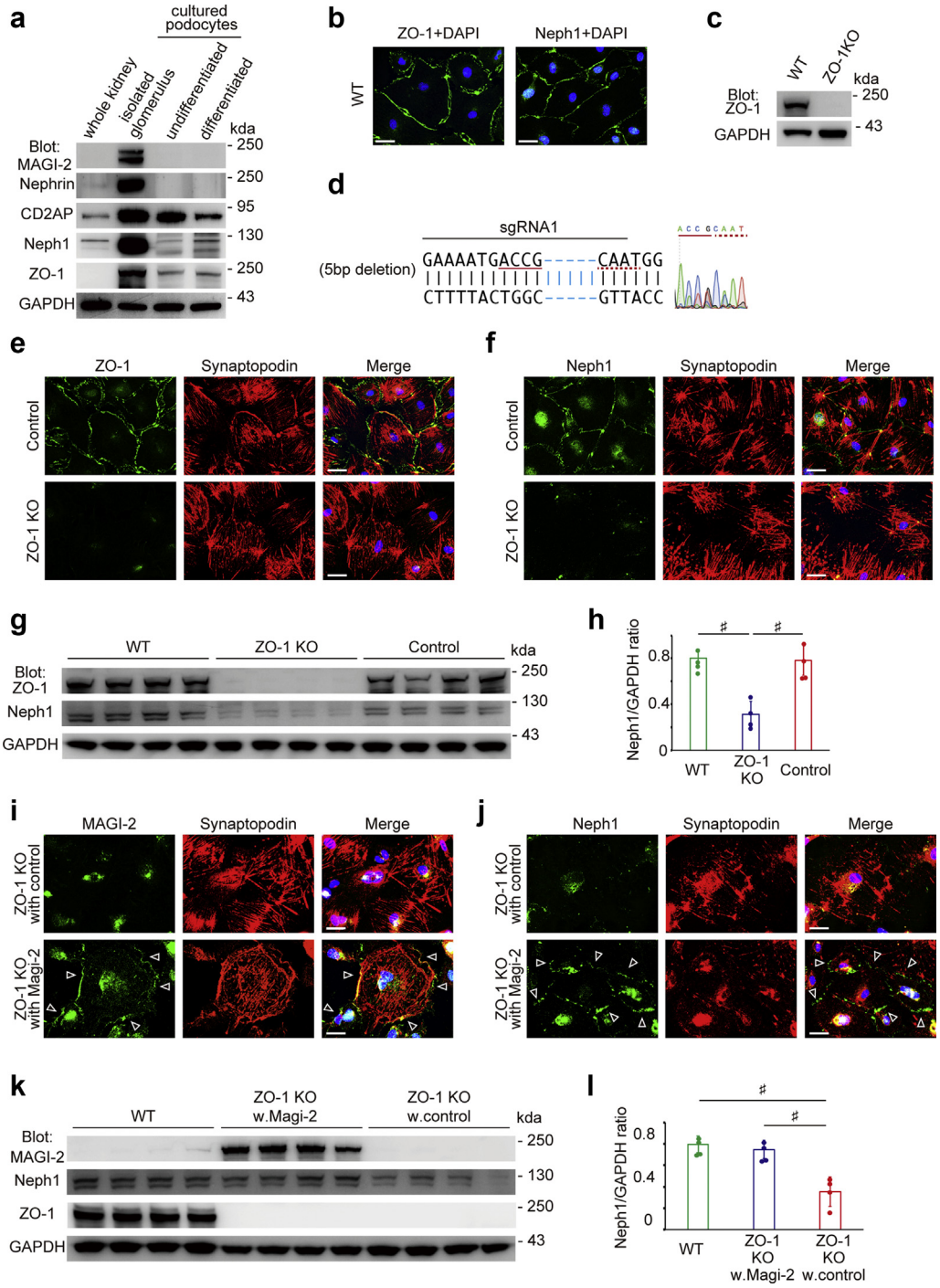

Figure 3 | MAGI-2 localizes Neph1 to the cellular edge in cultured podocytes. (**a**) Western blot analysis for MAGI-2, nephrin, CD2AP, neph1, and ZO-1 expression in whole kidney, isolated glomerulus, undifferentiated, and differentiated cultured podocytes. (**b**) Representative immunofluorescence images of neph1, ZO-1 (green), and DAPI (blue) in cultured WT podocytes. Bar = 30 μm. (c) Western blot analysis for ZO-1 expression of WT and ZO-1 KO podocytes. (**d**) Sanger sequence analysis of cultured ZO-1 KO podocytes. (**e**) Representative immunofluorescence images of ZO-1 (green) and synaptopodin (red) in cultured WT and ZO-1 KO podocytes. Bar = 30 μm. (**f**) Representative immunofluorescence images of neph1 (green) and synaptopodin (red) in cultured WT and ZO-1 KO podocytes. Bar = 30 μm. (**g**) Western blot analysis for ZO-1 and neph1 expression in cultured WT, ZO-1 KO, and CRISPR control podocytes. The 4 lanes in cultured ZO-1 KO podocytes are sgRNA 1-1, 1-2, 2, and 3 from left to right. Cultured WT CRISPR control podocytes are from the same clone. (**h**) Quantification of neph1 expression in the Western blot for WT, ZO-1 KO, and CRISPR control podocytes; $^{\#}P < 0.01$. (**i**) Representative immunofluorescence images of MAGI-2 (green) and synaptopodin (red) in cultured ZO-1 KO podocytes transfected with control or MAGI-2. The arrowheads indicate the MAGI-2 staining. Bar = 30 μm. (**j**) Representative immunofluorescence images of neph1 (green) and synaptopodin (red) in cultured ZO-1 KO podocytes transfected with control or MAGI-2. The arrowheads indicate the neph1 staining in cellular (continued)

MAGI-2 interacts with neph1 through PDZ 1 and 5

These results showed that MAGI-2 also functions as a scaffold protein of neph1 in a manner similar to that of ZO-1. To examine how MAGI-2 interacts with neph1, we next conducted a pull-down assay. Endogenous neph1 in glomerular lysate specifically attached to glutathione S-transferase (GST)-MAGI-2, but not to GST alone (Figure 4a). This result demonstrated that MAGI-2 also interacts with neph1 in podocytes.

Next, to examine which domain of each molecule is necessary for the binding between MAGI-2 and cytoplasmic neph1, we used a FLAG-tagged MAGI-2 and a green fluorescent protein (GFP)-tagged cytoplasmic region wild type (CR-WT) of neph1 (Figure 4b and c) to conduct co-immunoprecipitation (co-IP) experiments with human embryonic kidney T antigen (HEK 293T) cells. The co-IP experiments demonstrated the binding between neph1 and MAGI-2 (Figure 4d). Although we exchanged the tag of both molecules and retried co-IP, the results were similar (Supplementary Figure S6A). In addition, the cytoplasmic mutated neph1 T876K (CR-T786K) did not bind to MAGI-2 (Figure 4e). These results demonstrated that the PDZ binding motif of neph1 is essential for the binding to MAGI-2. To clarify which domain of MAGI-2 is necessary for binding to the cytoplasmic region of neph1, we flagged each PDZ domain of MAGI-2 (Figure 4c). In addition to the full-length MAGI-2, PDZ domains 1 and 5 were also bound to the CR-WT of neph1 (Figure 4f). MAGI-2-ΔPDZ 1+5, however, did not bind to the CR-WT of neph1 (Figure 4g). These results demonstrated that MAGI-2 binds to the cytoplasmic C-terminus of neph1 via the PDZ domains 1 and 5.

To verify the importance of the MAGI-2 PDZ domains 1 and 5, we then transfected MAGI-2-ΔPDZ 1+5 to cultured ZO-1 KO podocytes via electroporation. In the transfected podocytes, the neph1 expression was not apparently elevated (Supplementary Figure S6B and C).

MAGI-2 overexpression could recruit nephrin to the plasma membrane in podocytes

Our results from MAGI-2 pdKO and IpdKO mice showed that the MAGI-2 deficiency altered the immunostaining pattern and expression of nephrin. However, it remains controversial whether MAGI-2 regulates the cellular localization of nephrin.[37,38] We examined the hypothesis using cultured podocytes and genome-editing technology. Because MAGI-2 and nephrin were not expressed in cultured podocytes (Figure 4a), we generated cultured MAGI-2 full-length overexpression podocytes and control podocytes via a piggyBac transposon system using 2 types of vectors (Figure 5a).[45] Immunofluorescence analysis showed that MAGI-2 was expressed at the cellular edge of cultured MAGI-2 overexpression podocytes, but not in control podocytes (Figure 5b). Western blots also supported the immunofluorescence results (Figure 5c).

To examine the interaction between nephrin and MAGI-2, we then transfected either Myc-tagged nephrin full-length or control vector to the established cell lines using electroporation. Western blot of these cell lysates demonstrated the successful transfection to these cell lines (Figure 5d). Immunofluorescence of the transfected cells showed that in control groups, nephrin was not expressed at the cellular edge, but in MAGI-2 overexpression podocytes, nephrin could be localized at the cellular edge (Figure 5e). These results demonstrated that the overexpression of MAGI-2 in this context is sufficient to recruit nephrin to the plasma membrane.

MAGI-2 interacts with the C-terminus of nephrin through PDZ 3-5

Thus far, our results have demonstrated that MAGI-2 regulates the localization of nephrin. To examine how MAGI-2 interacts with nephrin, we performed a GST pull-down assay. Endogenous nephrin in glomerular extracts would specifically bind to GST-MAGI-2, but not to GST alone (Figure 6a). This result showed that MAGI-2 binds to nephrin.

To identify which domain in each molecule is necessary for the binding between MAGI-2 and nephrin, we performed co-IP experiments with a GFP-tagged cytoplasmic region wild type (CR-WT) of nephrin and a FLAG-tagged MAGI-2 (Figure 6b). The FLAG-MAGI-2 bound to GFP-nephrin CR-WT (Figure 6c). Reverse co-IP also showed similar binding (Supplementary Figure S7A). Nephrin has an atypical PDZ domain-binding motif sequence in its C-terminus. To determine whether the C-terminus of nephrin mediates the binding to MAGI-2, a nephrin construct was generated lacking all 4 amino acids in the C-terminus (CR-ΔGHLV). In contrast to GFP-nephrin CR-WT, the GFP-nephrin CR-ΔGHLV did not bind to FLAG-MAGI-2 (Figure 6d), indicating that nephrin binds to MAGI-2 via the GHLV sequence. Next, to map the domains in MAGI-2 responsible for the binding to nephrin, we used 6 MAGI-2 deletion constructs coding PDZ domains 0, 1, 2, 3, 4, and 5 and performed co-IP experiments in HEK 293T cells (Figure 6e). We found that GFP-nephrin CR-WT was co-precipitated with FLAG-MAGI-2-ΔPDZ0, -ΔPDZ1, -ΔPDZ2, and -ΔPDZ4, suggesting that PDZ3 and PDZ5 are essential for binding to nephrin (Figure 6f). Meanwhile, GFP-nephrin CR-WT did not co-precipitate with the FLAG-MAGI-2-single PDZ domain

Figure 3 | (continued) edge contact. Bar = 30 μm. (**k**) Western blot analysis for MAGI-2, neph1, and ZO-1 expression in cultured ZO-1 KO podocytes transfected with control or MAGI-2. The 4 lanes in cultured ZO-1 KO podocytes are sgRNA 1-1, 1-2, 2, and 3 from left to right. The actual sequence of each sgRNA is described in Supplementary Figure S8. Cultured WT podocytes are from the same clone. (**l**) Quantification of neph1 expression in the western blot for WT, ZO-1 KO, and CRISPR control podocytes; $^{\#}P < 0.01$. CD2AP, CD2 associated protein; CRISPR, clustered regularly interspaced short palindromic repeats; DAPI, 4′,6-diamidino-2-phenylindole; GAPDH, glyceraldehyde-3-phosphate dehydrogenase; KO, knockout; MAGI-2 pdKO, MAGI-2 podocyte-specific knockout; sgRNA, single-guide RNA; WT, wild type; ZO-1, zonula occludens-1. To optimize viewing of this image, please see the online version of this article at www.kidney-international.org.

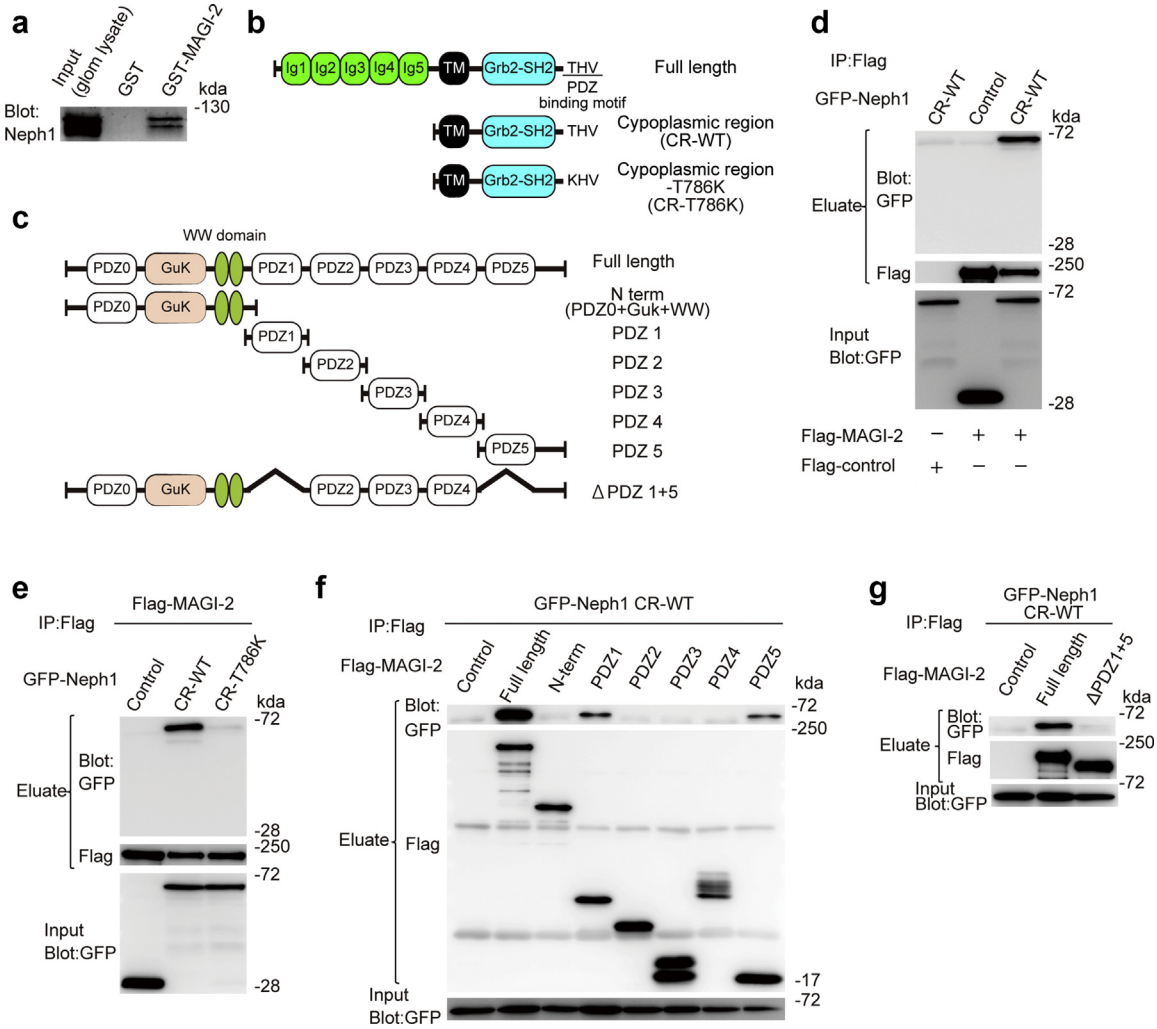

Figure 4 | MAGI-2 interacts with neph1 through PDZ domains 1 and 5. (**a**) GST pull-down assay to determine the binding between MAGI-2 and neph1 in podocytes. (**b**) Schematic presentation of the neph1 structure used in this study. (c) Schematic presentation of the MAGI-2 structure used in this study. (**c**) Flag-MAGI-2 binds to GFP-neph1 cytoplasmic region wild type (CR-WT). (**d–g**) Immunoblots of immunoprecipitation experiments of HEK 293T cells transfected with FLAG-MAGI-2 and the CR-WT of GFP-neph1. (**d**) Mutated neph1 T786K does not bind to MAGI-2. (**f**) PDZ 1 or 5 alone in MAGI-2 could bind to neph1. (**g**) Deletion of PDZ 1 and the 5 domain in MAGI-2 prevents binding to neph1. GFP, green fluorescent protein; GST, glutathione S-transferase; GuK, guanylate kinase; Ig, immunoglobulin; IP, immunoprecipitation; SH-2, Src homology 2 domain; TM, transmembrane; WW, WWP repeating motif.

(-N-term [including PDZ 0], -PDZ1, -PDZ2, -PDZ3, -PDZ4, and -PDZ5) (Figure 6g and Supplementary Figure S7B). We hypothesized that nephrin requires multiple PDZ domains for binding to MAGI-2. Further co-IP experiments showed that GFP-nephrin CR-WT co-precipitated with FLAG-MAGI-2-PDZ3-5 but not with either -PDZ3+4 or -PDZ4+5 (Figure 6h and Supplementary Figure S7B). These results demonstrated that the C-terminus 4 amino acids of cytoplasmic nephrin bind entirely to the PDZ3-5 domains on MAGI-2.

Based on these results, we have generated cultured MAGI-2 ΔPDZ 3-5 overexpression podocytes and transfected nephrin via electroporation (Supplementary Figure S7C). In the overexpression podocytes, the truncated MAGI-2 expression was not detected in the cellular edge, unlike MAGI-2 full-length overexpression podocytes (Figure 5c and Supplementary Figure S7D). Nephrin was expressed mainly in the cell body of the cultured podocytes (Supplementary Figure S7D). It also supported the above co-IP results.

MAGI-2 expression is associated with the localization and expression of SD in human glomerular diseases

These analyses demonstrated that MAGI-2 regulates the localization of the key SD components with binding via PDZ domains. To assess the importance of MAGI-2 in human glomerular diseases, we stained human biopsy samples with MAGI-2. In glomerular diseases with glomerulosclerosis such as FSGS or IgA nephropathy (bad prognosis), the immunofluorescence intensity of MAGI-2 was relatively weaker compared with other glomerular diseases (Figure 7a). Quantification of the intensity presented similar results (Figure 7b).

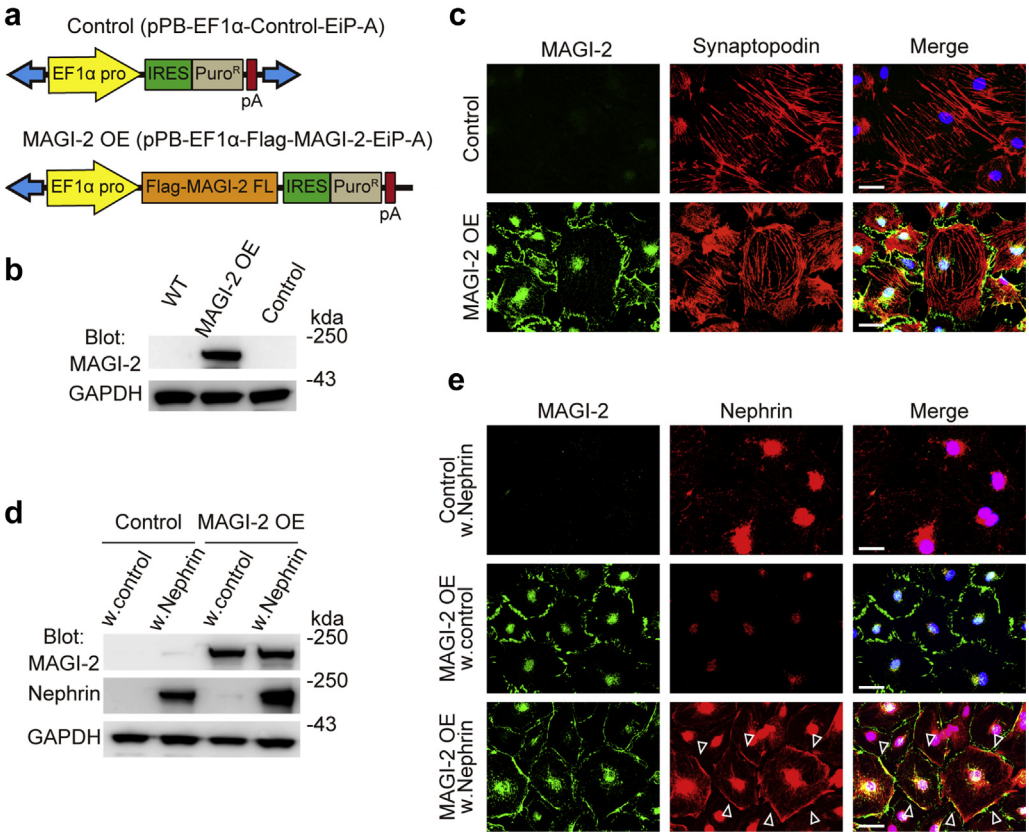

Figure 5 | MAGI-2 tethers nephrin to plasma membrane in cultured podocytes through PDZ domains. (**a**) Schematic presentation of transfected plasmid DNA: pPB- EF1α-control-iP-A for cultured control podocytes and pPB-EF1α-Flag-MAGI-2-iP-A for cultured MAGI-2 overexpression podocytes. (**b**) Western blot analysis for MAGI-2 expression in cultured WT, MAGI-2 OE, and control podocytes. (**c**) Representative immunofluorescence images of MAGI-2 (green) and synaptopodin (red) in cultured control and MAGI-2 overexpression podocytes. Bar = 30 μm. (**d**) Western blot analysis for MAGI-2 and nephrin expression in cultured control and MAGI-2 overexpression podocytes transfected with control or nephrin. (**e**) Representative immunofluorescence images of MAGI-2 (green) and nephrin (red) in cultured control and MAGI-2 overexpression podocytes transfected with control empty vector or nephrin. The arrowheads indicates the nephrin staining at the cellular edge. Bar = 30 μm. FL, full length; GAPDH, glyceraldehyde-3-phosphate dehydrogenase; IRES, internal ribosome entry site; OE, overexpression; PB, piggyBac; Puro, puromycin; WT, wild type. To optimize viewing of this image, please see the online version of this article at www.kidney-international.org.

The staining pattern of nephrin was also altered, depending on the MAGI-2 expression in the glomeruli. In minor glomerular abnormalities, the staining pattern of nephrin retained a capillary pattern that was similar to that of control mice and rats (Figure 7c). Meanwhile, much higher magnification also showed that in FSGS and IgA nephropathy (bad prognosis), the nephrin staining pattern became cytosolic mainly in the area where the MAGI-2 expression disappeared. As for neph1 staining, the immunofluorescence intensity coincides with the MAGI-2 expression. These results indicated that MAGI-2 is also downregulated in human glomerular diseases with glomerulosclerosis. It also suggests that the decreased expression of MAGI-2 could be associated with the altered localization and expression of nephrin and neph1.

DISCUSSION

Because nephrin and neph1 are the main components of the SD of podocytes, it is highly desirable to elucidate the molecular mechanism of how the localization of these backbone proteins is stabilized in podocytes. Meanwhile, MAGI-2 is among the multidomain scaffold proteins that are expressed in podocytes.[26,27] As the previous studies showed, the function of MAGI-2 for the SDs remains obscure.[28] Our study has shown that MAGI-2 orchestrates the localization of nephrin and neph1 through PDZ domains together with other scaffold proteins (Figure 8). In other words, MAGI-2 plays a critical role in stabilizing the glomerular filtration barrier as a scaffold protein.

Previously we demonstrated that MAGI-2 also interacts with dendrin, which is 1 of the key molecules in podocyte apoptosis.[32] We also showed that MAGI-2 interferes with podocyte apoptosis by preventing the nuclear translocation of dendrin. Recent basic and clinical research has also indicated that the nuclear translocation of dendrin induces podocyte apoptosis.[46–49] In addition, other groups also demonstrated that MAGI-2 is a key molecule of Rap1 signaling, which is related to actin remodeling and secretion.[27] Taken together, MAGI-2 has 3 important functions for maintaining the filtration barrier: preventing podocyte apoptosis, regulating

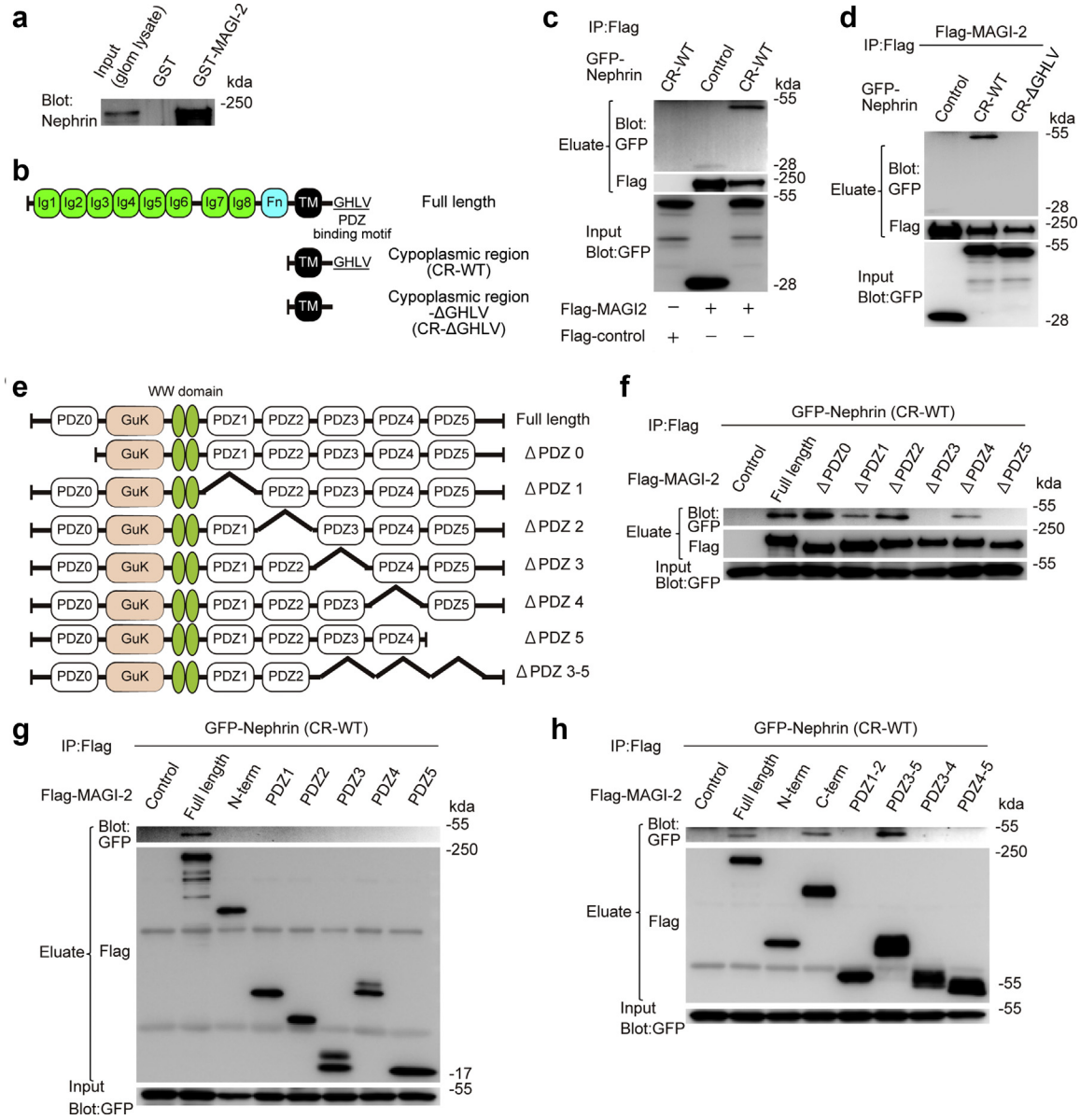

Figure 6 | MAGI-2 binds to nephrin via PDZ domains 3-5. (**a**) GST pull-down assay to determine the interaction between MAGI-2 and nephrin in podocytes. (**b**) Schematic presentation of the nephrin structure used in this study. (**c**,**d**,**f**–**h**) Immunoblots of immunoprecipitation experiments of 293T cells transfected with Flag-MAGI-2 and GFP-nephrin CR-WT. (**c**) Flag-MAGI-2 interacts with GFP-nephrin CR-WT. (**d**) Truncation of amino acid GHLV in nephrin C-terms interferes with the binding between MAGI-2 and nephrin. (**e**) Schematic presentation of the MAGI-2 structure used in this study. (**f**) Deletion of PDZ 3 and PDZ 5 domains in MAGI-2 interferes with the binding between MAGI-2 and nephrin. (**g**) Each PDZ domain alone in MAGI-2 does not bind to nephrin. (h) Consecutive PDZ 3-5 domains in MAGI-2 bind to nephrin, whereas neither the PDZ 3-4 domain nor the 4-5 domain does. CR-WT, cytoplasmic regions wild type; FN, fibronectin type III domain; GFP, green fluorescent protein; GHLV, 4 amino acids in the C-terminus; GST, glutathione S-transferase; GuK, guanylate kinase; Ig, immunoglobulin; TM, transmembrane; WW, WWP repeating motif.

Rap1 signaling, and stabilizing SD proteins. Therefore, the absence of MAGI-2 results in severe proteinuria and glomerulosclerosis.

The importance of PDZ domains in MAGI-2 is highlighted not only by our study in mice, but also by other reverse genetic studies in patients with nephrotic syndrome.[30,35,36] Ashraf *et al.*[30] performed homogenous mapping combined with whole-exome sequencing in familial nephrotic syndrome. They identified 2 homozygous mutations in the *MAGI-2* genes of patients with steroid-refractory nephrotic syndrome. The mutations induced a premature stop codon in the upstream of PDZ domain 4 of the *MAGI-2* gene. Bierzynska *et al.*[35] also performed whole-exome sequencing on a deeply phenotyped cohort of 187 patients with childhood steroid-refractory nephrotic syndrome. Their analysis revealed a frame shift mutation in the PDZ domain 5 sequence of the *MAGI-2* gene in patients. Thus, these human genome studies indicated the importance of PDZ domains 4-5 in the *MAGI-2* gene, and our study also demonstrated that PDZ domains 3-5 are crucial for interacting with SD proteins.

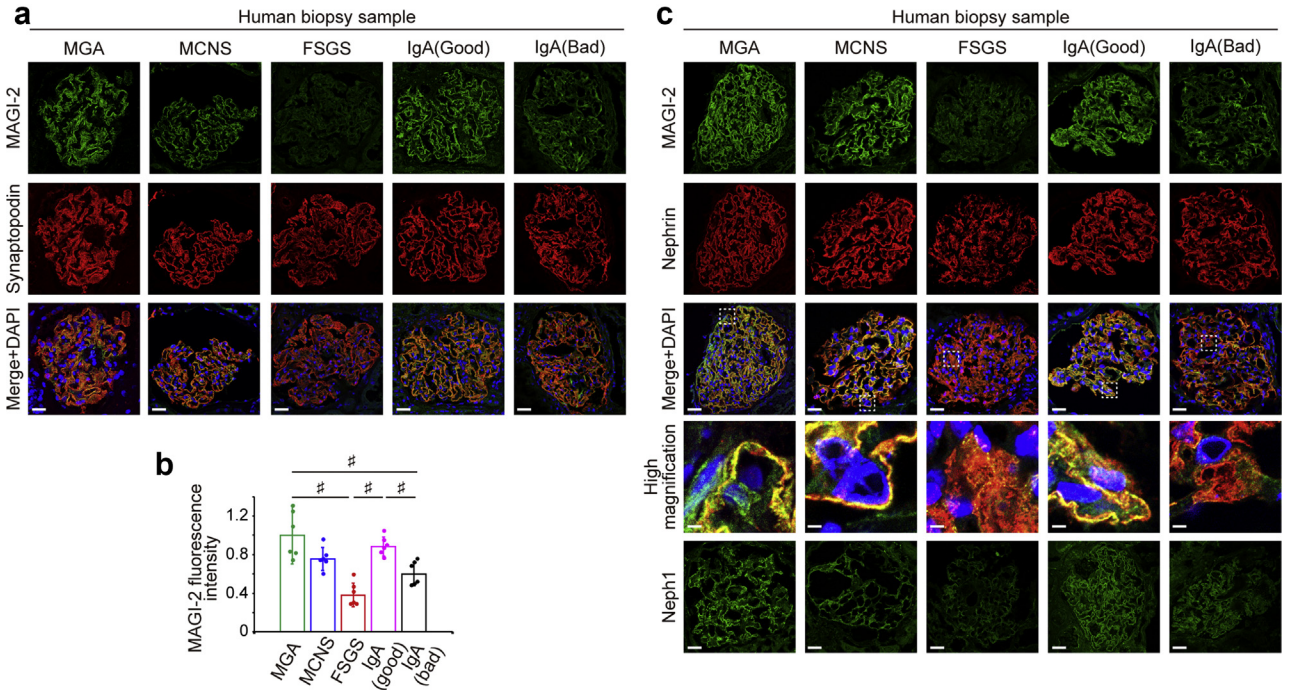

Figure 7 | MAGI-2 expression is associated with the localization and expression of nephrin and neph1 in human glomerular disease. (**a**) Representative glomerular immunofluorescence images of MAGI-2 (green) and synaptopodin (red) in human glomerular diseases. Bar = 10 μm. (**b**) Quantification of immunofluorescence intensity of MAGI-2 in human glomerular diseases. $^{\#}P < 0.01$, by analysis of variance with Bonferroni correction. (**c**) Representative glomerular immunofluorescence images of MAGI-2 (green), nephrin (red), and Neph1(green) in human glomerular diseases. The white dotted boxes indicate high magnification. Bars = 1 μm and 10 μm. DAPI, 4′,6-diamidino-2-phenylindole; FSGS, focal segmental glomerulosclerosis; GFP, green fluorescent protein; MCNS, minimal change nephrotic syndrome; MGA, minor glomerular abnormalities. To optimize viewing of this image, please see the online version of this article at www.kidney-international.org.

Our results could suggest the molecular mechanism for the phenotype of MAGI-2 mutations in humans. We believe that further research into protecting the MAGI-2 expression could lead to a new route for new drug development against proteinuria.

As with MAGI-2, ZO-1 is known as a critical scaffold protein in podocytes. Previous studies showed that podocyte-specific ZO-1 KO mice exhibited severe glomerulosclerosis and demonstrated the interaction between ZO-1 and neph1.[23,42,50] Meanwhile, in our study, although the

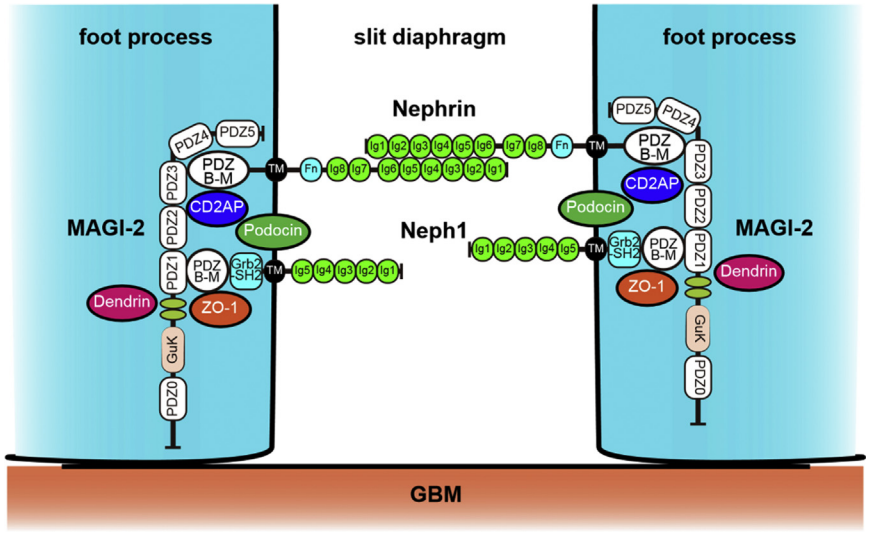

Figure 8 | Schematic presentation of slit diaphragm components and MAGI-2. B-M, binding motif; CD2AP, CD2 associated protein; GBM, glomerular basement membrane; ZO-1, zonula occludens-1.

ZO-1 expression was not reduced in MAGI-2 IpdKO and MAGI-2^{pdKO} mice, the neph1 expression was downregulated. In cultured ZO-1 KO podocytes, MAGI-2 could also reverse the reduced expression of neph1. These results show that both ZO-1 and MAGI-2 function as scaffold proteins in neph1. Furthermore, these results imply that, together, ZO-1 and MAGI-2 complement the assembly of neph1.

There are a few points on which our results disagree with the conclusions of previous studies. There are pros and cons concerning the interactions between nephrin and MAGI-2.[33,34,37,38] In our opinion, 1 of the possible reasons for this discrepancy is the molecular weight of MAGI-2. In the studies that agree with our results concerning the interaction between MAGI-2 and nephrin, the molecular weight of MAGI-2 was approximately 200 kDa.[33] In addition, most recent publications examining the function of MAGI-2 have also shown a similar molecular weight.[27,30] In another group, the molecular weight of purified MAGI-2 protein is listed at only 100 kDa.[38] In other words, the molecular weight of MAGI-2 in another group is materially short compared with that in our groups. We consider that this shortness of proteins could deeply influence the adhesion function of MAGI-2, as our cultured MAGI-2 ΔPDZ3-5 overexpression podocytes showed that the truncated MAGI-2 is not expressed in the cellular edge. Our studies also showed the co-localization of MAGI-2 and nephrin in cultured podocytes, whereas another group used other cultured cells.[38]

Our study has a few limitations. First, we did not demonstrate a direct interaction among nephrin, neph1, and MAGI-2. Therefore, we cannot rule out the possibility that other proteins may mediate these interactions. The second limitation concerns the MAGI-2 expression in cultured podocytes. Theoretically, MAGI-2 expression has been confirmed only in the cell-cell contact of cultured podocytes. Nevertheless, in our cultured podocytes, we could confirm the MAGI-2 expression not only in cell-cell contact but also in the cellular edge. Our possible reason for its expression is the extreme expression of MAGI-2 and the substantial electrical damage of electroporation. However, we believe that the immunostaining patterns of MAGI-2 did not necessarily deny our hypothesis. Preceding studies also showed a similar immunostaining pattern for MAGI-2 overexpression in cultured podocytes and COS7 cells.[31,51] Third, although we have demonstrated the interactions among nephrin, neph1, and MAGI-2 in a physiological state, we have not elucidated whether the interaction is regulated by factors such as stoichiometry, some crosstalk with other cells, or humoral factors. Fourth, although other groups have reported the association between MAGI-2 and Rap/GEF signaling, our studies have not examined these pathways using our MAGI-2 KO mice.[27] The fifth limitation concerns the specificty of our neph1 antibody. We suggest that our neph1 antibody has the appropriate function in terms of molecular weight and the staining pattern of glomeruli and cultured podocytes. However, as Figure 3b shows, our neph1 antibody stained a portion of nucleus in a similar fashion as that in preceding publications.[42,52,53] Therefore, we cannot deny the possibility that our neph1 antibody has little specificity.

CONCISE METHODS

Statistical analysis

All data are expressed as the mean ± SEM. Two sets of data were compared using an unpaired 2-tailed Student *t*-test. A P value <0.05 was considered statistically significant. When comparing more than 2 variables, a *t* test with Bonferroni correction was applied to prevent type I error. All statistical data were analyzed using JMP for Macintosh, version 10.0.2 software (SAS Institute, Tokyo, Japan).

Detailed methods, an antibody list, and primer information are described in the Supplementary Methods, Supplementary Table S1 and Table S2, respectively.

DISCLOSURE

All the authors declared no competing interest.

ACKNOWLEDGMENTS

We thank Lawrence B. Holzman (University of Pennsylvania) for the Neph2-cre mice and Pierre Chambon (University of Strasbourg) for the Nphs2-CreER^{T2} transgenic mice. We thank Yutaka Harita (University of Tokyo) for the neph1 construct and the neph1 antibody. We thank Chinatsu Toguchi, Chihiro Nakagawa, Yuri Ogawa, Chihiro Makino, and Mayu Miyaki for their excellent technical assistance. We thank Keiko Okamoto-Furuta and Haruyasu Kohda (Division of Electron Microscopic Study, Center for Anatomical Studies, Graduate School of Medicine, Kyoto University) for their skillful technical support with the electron microscopy. We thank Motoko Kimura, Kiyoshi Hirahara, and Toshinori Nakayama (Department of Immunology, Graduate School of Medicine, Chiba University) for their technical support with confocal microscopy. We thank Yurie Nakaya for kind support with the intellectual property. This work was supported in part by a Ministry of Education, Culture, Sports, Science and Technology of Japan Grant-in-Aid for Scientific Research 26670431, 17K19653, 18H02823 (KA). This research was also partially supported by the Japan Agency for Medical Research and Development under grants JP18gm5010002 and JP18gm0610011 (MY).

Outside the contents of the study, KA and MY have received research funding from Mitsubishi Tanabe Pharmaceutical Corporation.

AUTHOR CONTRIBUTIONS

HYa, NS, and KA conceived of the hypothesis, conducted the experiments, and wrote the manuscript. SM, TM, JAOT, KY-N, MKik, and MKim collaborated on the experiments. MAE and INK revised the manuscript. KI conducted the post-embedding immunoelectron microscopy. HYo and MM provided the NPHS2-CreER^{T2} mouse model. AH provided technical advice and the plasmid vectors. KN provided the MAGI-2$^{flox/flox}$ mouse model. MY supervised the experimental design and interpreted the results.

SUPPLEMENTARY MATERIAL

Supplementary File (PDF)

Supplementary Methods.

Figure S1. (**A**) Urinary albumin-to-creatinine ratio of control mice and Adriamycin-induced nephropathy mice. *$P < 0.05$. (**B**) Representative glomerular immunofluorescence images of MAGI-2 (green), synaptopodin (red), nephrin (green), and neph1 (green) in Adriamycin nephropathy mice. Bar = 20 μm. (**C**) Urinary albumin-to-creatinine ratio of control rat and puromycin nephropathy rat. *$P < 0.05$. (**D**) Representative glomerular immunofluorescence images of MAGI-2

(green), synaptopodin (red), nephrin (green), and neph1 (green) in puromycin nephropathy rat. Bar = 15 μm.

Figure S2. (**A**) Glomerulosclerosis index in control and MAGI-2 IpdKO mice 6 months after tamoxifen injection; *$P < 0.05$. (**B**) Representative glomerular immunofluorescence images of WT-1 in control and MAGI-2 IpdKO mice. (**C**) Quantification of WT-1 positive dots per glomerulus in control and MAGI-2 IpdKO mice; *$P < 0.05$.

Figure S3. (**A**) Representative immunofluorescence images of ZO-1 (green) and synaptopodin (red) in other cell lines of cultured ZO-1 KO podocytes; Bar = 30 μm. (**B**) Representative immunofluorescence images of neph1 (green) and synaptopodin (red) in other cell lines of cultured ZO-1 KO podocytes. Bar = 30 μm.

Figure S4. (**A**) Sanger sequence analysis of the off-target candidate sites in cultured ZO-1 KO podocytes. (**B**) Neph1 mRNA expression of wild type (WT), ZO-1 KO, and control by real-time PCR. (**C**) Degradation pathway analysis of neph1 protein expression in cultured ZO-1 KO podocytes. Bortezomib and E64d plus pepstatin A were administered for inhibiting ubiquitin-proteasome pathway and autophagy pathway, respectively.

Figure S5. (**A**) Representative images of cultured podocytes in which pCAG-EGFP were transfected with lipofection method and electroporation system.

Figure S6. (**A**) Immunoblots of immunoprecipitation experiments of 293T cells transfected with Flag-neph1 cytoplasmic regions and GFP-MAGI-2. (**B**) Representative immunofluorescence images of MAGI-2 (green), nehp1 (green), and synaptopodin (red) in cultured ZO-1 KO podocytes transfected with MAGI-2 ΔPDZ 1+5. The arrowheads indicate the MAGI-2 staining on cellular edge. Bar = 30 μm. (**C**) Western blot analysis for MAGI-2 and Neph1 expression in cultured ZO-1 KO podocytes transfected with MAGI-2 ΔPDZ 1+5.

Figure S7. (**A**) Immunoblots of immunoprecipitation experiments of 293T cells transfected with Flag-nephrin cytoplasmic regions and GFP-MAGI-2. (**B**) Schematic presentation of MAGI-2 that was used in this study. (**C**) Western blot analysis for MAGI-2 and nephrin expression in cultured MAGI-2 ΔPDZ 3-5 podocytes transfected with full-length nephrin. (**D**) Representative immunofluorescence images of MAGI-2 (green), nephrin (red) in cultured MAGI-2 ΔPDZ 3-5 overexpression podocytes transfected with full-length nephrin. Bar = 30 μm.

Figure S8. (**A**) Our guide RNA sequence for exon 4 in ZO-1. (**B**) T7 endonuclease 1 assay showed the cleavage efficiency of each guide RNA.

Table S1. Results of each electroporation condition.

Table S2. Antibody list used in this study.

Table S3. Primers list used in this study.

REFERENCES

1. Kawachi H, Miyauchi N, Suzuki K, et al. Role of podocyte slit diaphragm as a filtration barrier. *Nephrology (Carlton)*. 2006;11:274–281.
2. Grahammer F, Schell C, Huber TB. The podocyte slit diaphragm—from a thin grey line to a complex signalling hub. *Nat Rev Nephrol*. 2013;9:587–598.
3. Brinkkoetter PT, Ising C, Benzing T. The role of the podocyte in albumin filtration. *Nat Rev Nephrol*. 2013;9:328–336.
4. Butt L, Unnersjö-Jess D, Höhne M, et al. A molecular mechanism explaining albuminuria in kidney disease. *Nat Metab*. 2020;2:461–474.
5. Grahammer F, Wigge C, Schell C, et al. A flexible, multilayered protein scaffold maintains the slit in between glomerular podocytes. *JCI insight*. 2016;1:e86177.
6. Fogo AB. Causes and pathogenesis of focal segmental glomerulosclerosis. *Nat Rev Nephrol*. 2015;11:76–87.
7. Reiser J, Altintas MM. Podocytes. *F1000Res*. 2016;5:F100.
8. Kestila M, Lenkkeri U, Männikkö M, et al. Positionally cloned gene for a novel glomerular protein—nephrin—is mutated in congenital nephrotic syndrome. *Mol Cell*. 1998;1:575–582.
9. Donoviel DB, Freed DD, Vogel H, et al. Proteinuria and perinatal lethality in mice lacking NEPH1, a novel protein with homology to NEPHRIN. *Mol Cell Biol*. 2001;21:4829–4836.
10. Barletta GM, Kovari IA, Verma RK, et al. Nephrin and Neph1 co-localize at the podocyte foot process intercellular junction and form cis hetero-oligomers. *J Biol Chem*. 2003;278:19266–19271.
11. Santin S, Garcia-Maset R, Ruiz P, et al. Nephrin mutations cause childhood- and adult-onset focal segmental glomerulosclerosis. *Kidney Int*. 2009;76:1268–1276.
12. Machuca E, Benoit G, Nevo F, et al. Genotype-phenotype correlations in non-Finnish congenital nephrotic syndrome. *J Am Soc Nephrol*. 2010;21:1209–1217.
13. Trautmann A, Bodria M, Ozaltin F, et al. Spectrum of steroid-resistant and congenital nephrotic syndrome in children: the PodoNet registry cohort. *Clin J Am Soc Nephrol*. 2015;10:592–600.
14. Mohanapriya CD, Vettriselvi V, Nammalwar BR, et al. Novel variations in NPHS1 gene in children of South Indian population and its association with primary nephrotic syndrome. *J Cell Biochem*. 2018;119:10143–10150.
15. Solanki AK, Widmeier E, Arif E, et al. Mutations in KIRREL1, a slit diaphragm component, cause steroid-resistant nephrotic syndrome. *Kidney Int*. 2019;96:883–889.
16. Bonomo JA, Ng MC, Palmer ND, et al. Coding variants in nephrin (NPHS1) and susceptibility to nephropathy in African Americans. *Clin J Am Soc Nephrol*. 2014;9:1434–1440.
17. Zhuo L, Huang L, Yang Z, et al. A comprehensive analysis of NPHS1 gene mutations in patients with sporadic focal segmental glomerulosclerosis. *BMC Medl Genet*. 2019;20:111.
18. Yoshizawa C, Kobayashi Y, Ikeuchi Y, et al. Congenital nephrotic syndrome with a novel NPHS1 mutation. *Pediatr Int*. 2016;58:1211–1215.
19. Li GM, Cao Q, Shen Q, et al. Gene mutation analysis in 12 Chinese children with congenital nephrotic syndrome. *BMC Nephrol*. 2018;19:382.
20. Thi Kim Lien N, Van Dem P, Thu Huong N, et al. The role of p.Ser1105Ser (in *NPHS1* gene) and p.Arg548Leu (in *PLCE1* gene) with disease status of Vietnamese patients with congenital nephrotic syndrome: benign or pathogenic? *Medicina (Kaunas)*. 2019;55:102.
21. Shih NY, Li J, Cotran R, et al. CD2AP localizes to the slit diaphragm and binds to nephrin via a novel C-terminal domain. *Am J Pathol*. 2001;159:2303–2308.
22. Schwarz K, Simons M, Reiser J, et al. Podocin, a raft-associated component of the glomerular slit diaphragm, interacts with CD2AP and nephrin. *J Clin Invest*. 2001;108:1621–1629.
23. Huber TB, Schmidts M, Gerke P, et al. The carboxyl terminus of Neph family members binds to the PDZ domain protein zonula occludens-1. *J Biol Chem*. 2003;278:13417–13421.
24. Tossidou I, Teng B, Worthmann K, et al. Tyrosine phosphorylation of CD2AP affects stability of the slit diaphragm complex. *J Am Soc Nephrol*. 2019;30:1220–1237.
25. Yaddanapudi S, Altintas MM, Kistler AD, et al. CD2AP in mouse and human podocytes controls a proteolytic program that regulates cytoskeletal structure and cellular survival. *J Clin Invest*. 2011;121:3965–3980.
26. Hirao K, Hata Y, Ide N, et al. A novel multiple PDZ domain-containing molecule interacting with N-methyl-D-aspartate receptors and neuronal cell adhesion proteins. *J Biol Chem*. 1998;273:21105–21110.
27. Lehtonen S, Ryan JJ, Kudlicka K, et al. Cell junction-associated proteins IQGAP1, MAGI-2, CASK, spectrins, and alpha-actinin are components of the nephrin multiprotein complex. *Proc Natil Acad Sci U S A*. 2005;102:9814–9819.
28. Empitu MA, Kadariswantiningsih IN, Aizawa M, Asanuma K. MAGI-2 and scaffold proteins in glomerulopathy. *Am J Physiol Renal Phys*. 2018;315:F1336–F1344.
29. Hammad MM, Dunn HA, Ferguson SSG. MAGI proteins can differentially regulate the signaling pathways of 5-HT2AR by enhancing receptor trafficking and PLC recruitment. *Cell Signal*. 2018;47:109–121.
30. Ashraf S, Kudo H, Rao J, et al. Mutations in six nephrosis genes delineate a pathogenic pathway amenable to treatment. *Nat Commun*. 2018;9:1960.
31. Zhu B, Cao A, Li J, et al. Disruption of MAGI2-RapGEF2-Rap1 signaling contributes to podocyte dysfunction in congenital nephrotic syndrome caused by mutations in MAGI2. *Kidney Int*. 2019;96:642–655.
32. Shirata N, Ihara KI, Yamamoto-Nonaka K, et al. Glomerulosclerosis Induced by deficiency of membrane-associated guanylate kinase inverted 2 in kidney podocytes. *J Am Soc Nephrol*. 2017;28:2654–2669.

33. Balbas MD, Burgess MR, Murali R, et al. MAGI-2 scaffold protein is critical for kidney barrier function. *Proc Natl Acad Sci U S A*. 2014;111:14876–14881.
34. Lefebvre J, Clarkson M, Massa F, et al. Alternatively spliced isoforms of WT1 control podocyte-specific gene expression. *Kidney Int*. 2015;88:321–331.
35. Bierzynska A, Soderquest K, Dean P, et al. MAGI2 mutations cause congenital nephrotic syndrome. *J Am Soc Nephrol*. 2017;28:1614–1621.
36. Zuo Z, Shen JX, Pan Y, et al. Weighted gene correlation network analysis (WGCNA) detected loss of MAGI2 (CKD) by podocyte damage promotes chronic kidney disease. *Cell Physiol Biochem*. 2018;51:244–261.
37. Hirabayashi S, Mori H, Kansaku A, et al. MAGI-1 is a component of the glomerular slit diaphragm that is tightly associated with nephrin. *Lab Invest*. 2005;85:1528–1543.
38. Weng Z, Shang Y, Ji Z, et al. Structural basis of highly specific interaction between nephrin and MAGI1 in slit diaphragm assembly and signaling. *J Am Soc Nephrol*. 2018;29:2362–2371.
39. Fogo AB. Animal models of FSGS: lessons for pathogenesis and treatment. *Semin Nephrol*. 2003;23:161–171.
40. Ihara K, Asanuma K, Fukuda T, et al. MAGI-2 is critical for the formation and maintenance of the glomerular filtration barrier in mouse kidney. *Am J Pathol*. 2014;184:2699–2708.
41. Yokoi H, Kasahara M, Mukoyama M, et al. Podocyte-specific expression of tamoxifen-inducible Cre recombinase in mice. *Nephrol Dial Transplant*. 2010;25:2120–2124.
42. Sagar A, Arif E, Solanki AK, et al. Targeting Neph1 and ZO-1 protein-protein interaction in podocytes prevents podocyte injury and preserves glomerular filtration function. *Sci Rep*. 2017;7:12047.
43. Wagner MC, Rhodes G, Wang E, et al. Ischemic injury to kidney induces glomerular podocyte effacement and dissociation of slit diaphragm proteins Neph1 and ZO-1. *J Biol Chem*. 2008;283:35579–35589.
44. Li HL, Gee P, Ishida K, Hotta A. Efficient genomic correction methods in human iPS cells using CRISPR-Cas9 system. *Methods (San Diego, Calif)*. 2016;101:27–35.
45. Matsui H, Fujimoto N, Sasakawa N, et al. Delivery of full-length factor VIII using a piggyBac transposon vector to correct a mouse model of hemophilia A. *PloS One*. 2014;9:e104957.
46. Schwartzman M, Reginensi A, Wong JS, et al. Podocyte-specific deletion of Yes-associated protein causes FSGS and progressive renal failure. *J Am Soc Nephrol*. 2016;27:216–226.
47. Lin T, Zhang L, Liu S, et al. WWC1 promotes podocyte survival via stabilizing slit diaphragm protein dendrin. *Mol Med Rep*. 2017;16:8685–8690.
48. Mizdrak M, Vukojevic K, Filipovic N, et al. Expression of DENDRIN in several glomerular diseases and correlation to pathological parameters and renal failure—preliminary study. *Diagn Pathol*. 2018;13:90.
49. Weins A, Wong JS, Basgen JM, et al. Dendrin ablation prolongs life span by delaying kidney failure. *Am J Pathol*. 2015;185:2143–2157.
50. Itoh M, Nakadate K, Horibata Y, et al. The structural and functional organization of the podocyte filtration slits is regulated by Tjp1/ZO-1. *PloS One*. 2014;9:e106621.
51. Sumita K, Sato Y, Iida J, et al. Synaptic scaffolding molecule (S-SCAM) membrane-associated guanylate kinase with inverted organization (MAGI)-2 is associated with cell adhesion molecules at inhibitory synapses in rat hippocampal neurons. *J Neurochem*. 2007;100:154–166.
52. Arif E, Wagner MC, Johnstone DB, et al. Motor protein Myo1c is a podocyte protein that facilitates the transport of slit diaphragm protein Neph1 to the podocyte membrane. *Mol Cell Biol*. 2011;31:2134–2150.
53. Kim EY, Chiu YH, Dryer SE. Neph1 regulates steady-state surface expression of Slo1 Ca(2+)-activated K(+) channels: different effects in embryonic neurons and podocytes. *Am J Physiol Cell Physiol*. 2009;297:C1379–C1388.